

propagating waveguide field, respectively. $\hat{c}^\dagger(\hat{c})$, $\hat{b}^\dagger(\hat{b})$, and $\hat{c}_{\text{in}}^\dagger(\hat{c}_{\text{in}})$ are the corresponding creation (annihilation) operators. L is the length of the waveguide and $\tilde{n}_g(y) = \frac{1}{L} \int_L n_g(x, y) dx$ denotes the perturbed group index of the waveguide optical mode $n_g(x, y)$. The fourth term describes the transport of photons from the waveguide to the cavity, or the “driving term.” $\gamma_e(y)$ is the cavity-waveguide decay (coupling) rate which is dependent on the position of the waveguide. In systems considered previously in the literature, the driving term was thought to be independent of displacement. This approximation, however, is only valid in very weakly coupled systems. Nevertheless, as we elucidate later, it is an important term and its displacement dependence can generally not be ignored. The remaining terms in Eq. (1) describe the intrinsic damping of the optical modes and the mechanical modes. At a small displacement y , the Hamiltonian can be linearized to the first order of y , yielding an optomechanical coupling Hamiltonian:

$$H_{\text{int}}/\hbar = \hat{y}[g_{\text{om}}\hat{c}^\dagger\hat{c} + k_{\text{om}}\hat{c}_{\text{in}}^\dagger\hat{c}_{\text{in}} + i\gamma_{\text{om}}\sqrt{1/2\gamma_e}(\hat{c}^\dagger\hat{c}_{\text{in}} - \hat{c}_{\text{in}}^\dagger\hat{c})]. \quad (2)$$

Here $g_{\text{om}} = \partial\omega_0/\partial y$ is the dispersive coupling coefficient, and $k_{\text{om}} = (\omega/c)(\partial\tilde{n}_g/\partial y)$ is the perturbation of the waveguide mode as described in [16]. Additionally, we introduce a new coupling term $\gamma_{\text{om}} = \partial\gamma_e(y)/\partial y$ to describe the optomechanical coupling between the cavity mode and the external waveguide mode. This coupling is of reactive nature since its expression is imaginary, resembling the similar coupling effects in other resonator systems [17]. Essentially we have identified a practical device system, in which the cavity is coupled to a bosonic environment—a single-mode waveguide channel in our case [12]. Both the dispersive coupling and the reactive coupling coefficients can be traced back to the evanescent overlap of the optical modes in the microdisk and the waveguide.

The quantum dynamics of the interaction Hamiltonian have been fully discussed by Elste *et al.* [12]. It was predicted that if the reactive term is significantly large, the quantum noises arising from these two sources of backaction could produce destructive interference, leading to a zero-temperature bath that allows optomechanical cooling without requiring the cavity to be in the good cavity limit. Although a full demonstration of ground state cooling remains difficult to achieve and requires cryogenic precooling, our goal here is to derive the optical force one would expect from such a dually coupled system and quantify the relevant coupling constants. The backaction force can be derived from Eq. (2):

$$\begin{aligned} \hat{F} &= -(d/dy)H_{\text{int}} \\ &= g_{\text{om}}\hat{c}^\dagger\hat{c} + k_{\text{om}}\hat{c}_{\text{in}}^\dagger\hat{c}_{\text{in}} + i\gamma_{\text{om}}\sqrt{1/2\gamma_e}(\hat{c}^\dagger\hat{c}_{\text{in}} - \hat{c}_{\text{in}}^\dagger\hat{c}). \end{aligned} \quad (3)$$

Instead of studying the fluctuations of the relevant operators, we calculate their steady-state values to yield the corresponding optical force. To this end, we look for the steady-state solution of the quantum Langevin equations:

$$\begin{aligned} \partial_t\hat{c} &= i(\omega - \omega_c - g_{\text{om}}y)\hat{c} - (\gamma_i + \gamma_e)\hat{c} + \sqrt{2\gamma_e}\hat{c}_{\text{in}}, \quad (4) \\ \partial_t\hat{p}_y &= -m\omega_M^2\hat{y} - \hbar g_{\text{om}}\hat{c}^\dagger\hat{c} \\ &\quad - i\gamma_{\text{om}}\sqrt{1/2\gamma_e}(\hat{c}^\dagger\hat{c}_{\text{in}} - \hat{c}_{\text{in}}^\dagger\hat{c}) - \gamma_M\hat{p}_y, \end{aligned} \quad (5)$$

where γ_i is the intrinsic damping rate of the cavity, and the Brownian noise term has been omitted. \hat{p}_y is the momentum of mechanical resonator. In the above equations, the driving term $\hat{c}_{\text{in}}^\dagger(\hat{c}_{\text{in}})$ is characterized by the steady-state average amplitude $E = \sqrt{P_{\text{in}}/\hbar\omega}$. The stationary solution is given by $c_s = \sqrt{2\gamma_e}E_{\text{in}}/(\gamma_e + \gamma_i - i(\omega - \omega_c))$. Then, the steady-state force F_s can be written as

$$F_s = -\hbar g_{\text{om}}|c_s|^2 - i\hbar\gamma_{\text{om}}\sqrt{1/2\gamma_e}c_{\text{in}}(c_s^* - c_s) - k_{\text{om}}|c_s|^2. \quad (6)$$

Therefore, the total optical force on the waveguide has three components. The first force term is associated with the backaction resulting from the intracavity photon energy change,

$$F_{\text{cav}} = -\hbar g_{\text{om}}|c_s|^2 = -\frac{P_{\text{in}}g_{\text{om}}}{\omega} \frac{2\gamma_e}{\Delta^2 + \gamma^2}, \quad (7)$$

where $\gamma = \gamma_e + \gamma_i$ is the half linewidth of the optical resonance and $\Delta = \omega - \omega_c$ is the cavity detuning. When the waveguide moves towards the disk (reducing y), the resonance frequency will decrease. Therefore we have $g_{\text{om}} = \partial g/\partial y > 0$. Hence, $F_{\text{cav}} < 0$ and this attractive force pulls the waveguide towards the microdisk. This is radically different from the radiation pressure force in a Fabry-Perot cavity which only pushes the mirror [18].

The second force term stems from the reactive coupling between the waveguide and the cavity:

$$F_{\text{reactive}} = -\frac{P_{\text{in}}\gamma_{\text{om}}}{\omega} \frac{2\Delta}{\Delta^2 + \gamma^2}. \quad (8)$$

When the waveguide moves toward the disk, the waveguide coupling rate γ_e will increase so $\gamma_{\text{om}} = \partial\gamma_e/\partial y < 0$. Therefore, this reactive force is attractive and enhances the aforementioned dispersive force when the cavity is red detuned ($\Delta < 0$); when the cavity is blue detuned ($\Delta > 0$), the reactive force is repulsive and partially cancels the dispersive optical force.

The third term $F_{\text{ev}} = -k_{\text{om}}P_{\text{in}}/\omega$ constitutes a constant gradient optical force resulting from the perturbed waveguide mode due to the presence of the microdisk, which is discussed in detail elsewhere [19]. This is a broadband background force that is independent of cavity detuning and does not directly impact the cavity dynamics.

Thus, the total force applied to the waveguide normalized to the input power is given by

$$f_{\text{total}} = f_{\text{cav}} + f_{\text{reactive}} + f_{\text{ev}} \\ = -\frac{2}{\omega\gamma^2} \frac{g_{\text{om}}\gamma_e + \gamma_{\text{om}}\gamma\varphi}{1 + \varphi^2} + f_{\text{ev}}, \quad (9)$$

where we define the normalized detuning $\varphi = \Delta/\gamma$. Further, if the cavity is in the so-called “critical coupling” condition, meaning that the transmission extinction ratio is maximal, $\gamma_e \approx \gamma_i \approx \gamma/2$, the expression for the force can be simplified to

$$f_{\text{total}} = -\frac{g_{\text{om}} + 2\gamma_{\text{om}}\varphi}{\omega\gamma(1 + \varphi^2)} + f_{\text{ev}}. \quad (10)$$

We fabricate the devices shown in Fig. 1 on silicon-on-insulator (SOI) wafers with 220 nm thick silicon layer and 3 μm thick buried oxide layers. The microdisk resonator has a radius of 40 μm . A freestanding waveguide (10 μm long and 300 nm wide), released from the substrate, is supported by two single-sided photonic crystal waveguide structures [8]. The gap between the waveguide and the disk is 250 nm. Light from a tunable diode laser is coupled in and out of the waveguide via two grating couplers with coupling efficiency of 10% each. Figure 2(a) shows the measured transmission spectrum of the device. A number of optical resonances can be observed, with a highest extinction ratio of up to 30 dB and quality factor of 120 000. At the resonance with very high extinction ratio as in Fig. 2(b), the coupling between the waveguide and the microdisk are impedance matched and the system can be approximated to be in the “critical coupling” condition. The optical force between the microdisk and the waveguide is described by Eq. (10). If the intensity of the light is modulated, the generated dynamic force will actuate the vibrant mechanical motion of the waveguide. In a pump-probe scheme, we use another probe light at a fixed wavelength, properly detuned from the resonance near 1559.00 nm, to measure the waveguide’s motion [19]. The actuation light wavelength is detuned from the resonance near 1564.25 nm. The input optical power of both the probe and actuation light is kept low at 20 μW (after compensating for the loss occurring at the input coupler) in order to avoid instability of the microdisk.

In Fig. 3, we show the measured resonance response of the waveguide with detuning $\varphi = \pm 1.0$, respectively. The

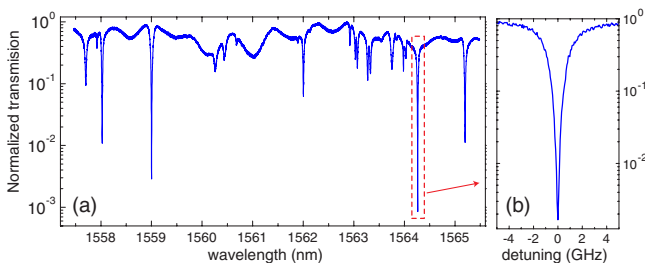


FIG. 2 (color online). Transmission spectrum of the microdisk resonator. The critically coupled mode was selected to demonstrate the reactive optical force.

waveguide is excited by the optical force into in-plane mechanical resonance with a frequency of 25.45 MHz and quality factor of 5000. It is notable that the phase of the response is reversed by π when the sign of φ is reversed. This indicates that the total force applied to the waveguide has changed direction from attractive ($\varphi = -1.0$) to repulsive ($\varphi = +1.0$), in accordance with our theoretical analysis from Eq. (10).

Because of the curvature of the disk, the distribution of the optical force on the beam is not uniform and has to be considered in the calculation of the effective mass m_{eff} for the fundamental mode, which is evaluated to be 0.6 of the physical mass m [18]. We then can determine both the magnitude and the direction of the optical force on the waveguide beam when the actuation laser is set to various detuning φ . The detailed force calibration process can be found in our prior publications [19]. The result is shown in Fig. 4. At large blue detuning, a repulsive gradient optical force is applied to the waveguide, while at red detuning, the sign of the force changes to be attractive. Counterintuitively, the total optical force is not maximal at zero detuning, in contrast to the radiation pressure force commonly encountered in Fabry-Perot cavity systems. Rather, the maximal repulsive or attractive optical force is obtained with detuning of $\varphi \sim \pm 1$, respectively.

The parameters g_{om} and γ_{om} can be found by fitting the result in Fig. 4(b) with Eq. (10). We found that $g_{\text{om}}/2\pi = 2.0 \pm 0.4$ MHz/nm and $\gamma_{\text{om}}/2\pi = -26.6 \pm 0.5$ MHz/nm. These values agree well with our numerical calculations results ($g_{\text{om}}/2\pi = 3.0$ MHz/nm and $\gamma_{\text{om}}/2\pi = -25$ MHz/nm) and values obtained with the method suggested in [18]. The static force F_{ev} unrelated to the cavity resonance is found to be attractive with a magnitude of -5.2 pN/mW, consistent with measured results when the actuation laser is tuned far away from the resonance. Thus the force F_{reactive} plays a dominant role in the current device system. According to Elste *et al.* [12], even though the system is not in the “good cavity limit,” it is possible to cool the waveguide’s mechanical mode to its ground state with the cavity backaction force at optimal detuning $\varphi_{\text{opt}} = \omega_M/2\gamma + g_{\text{om}}/\gamma_{\text{om}}$. Although direct cooling from

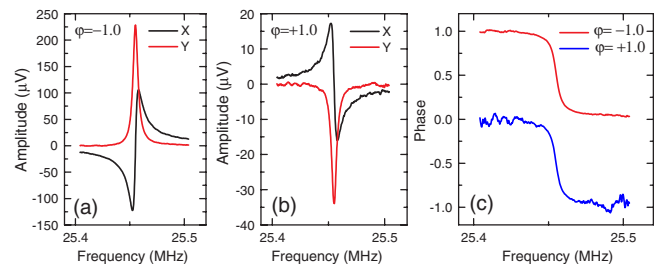


FIG. 3 (color online). Excited resonance response in X and Y quadrature of the waveguide resonator with detuning $\varphi = -1.0$ (a) and $\varphi = +1.0$ (b). In (c) the phase response for the two situations is shown. A phase shift of π , indicating the change of the direction of the optical force, is observed when the sign of detuning is reversed.

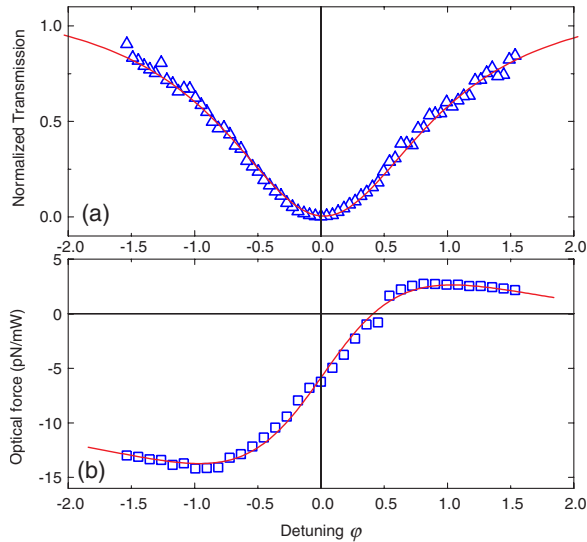


FIG. 4 (color online). The measured transmission (normalized) of the optical resonance (a) and the measured total optical force on the waveguide beam (b) versus detuning ϕ . The force is attractive at negative detuning ($\phi < 0$) and becomes repulsive at positive detuning ($\phi > 0.4$).

room temperature appears to be challenging (thermal occupation number $n_{\text{eq}} = k_B T / \hbar \omega_M = 250\,000$), with the recent demonstration of cryogenic precooling [4–6], reactive cooling will allow for backaction cooling to the ground state under practical experimental conditions and device parameters (precooling to 4.2 K, mechanical Q of 2×10^5 , optical Q of 5×10^5 and 5 mW input optical power at blue detuning $\Delta = 100$ MHz). We note that this blue-detuned ground state cooling is a result of destructive interference of the aforementioned two sources of quantum noises.

The identification of reactive cavity backaction is critical for the future development of strongly coupled cavity optomechanics [20]. It points to a new direction of ground state cooling without relying on reaching the “good cavity limit” (resolved side-band regime), which is a demanding requirement for nanoscale optomechanical systems. The relative strength of the reactive coupling and dispersive coupling coefficients (g_{om} and γ_{om}) largely depends on the size ratio of the resonator and waveguide. As long as the waveguide can carry a mode (and thus is a bosonic channel), the reactive coupling effect can not be ignored. However, if the waveguide is narrow enough so that it cannot carry a mode, the scenario changes to normal adiabatic resonator systems such as recently discussed in Ref. [18].

In conclusion, we have experimentally demonstrated spectrally tuned reactive cavity optical force in a cavity-waveguide device, which represents a practical, open cavity optomechanics system that couples to an external bosonic waveguide mode. A new type of reactive cavity backaction force is detected and quantified for the first time. We find that the dispersive optical force only constitutes a minor contribution to the total force.

We acknowledge a seedling grant from DARPA/MTO. W. H. P. P. acknowledges support from the Alexander von Humboldt Foundation. H. X. T. acknowledges a career grant from National Science Foundation and support from Yale Institute of Nanoscience and Quantum Engineering. The authors thank Steven Girvin for valuable discussions. The devices were fabricated at Yale University Center for Microelectronic Materials and Structures and the NSF-sponsored Cornell Nanoscale Facility.

*hong.tang@yale.edu

- [1] T.J. Kippenberg and K.J. Vahala, *Science* **321**, 1172 (2008).
- [2] T. Carmon, H. Rokhsari, L. Yang, T.J. Kippenberg, and K.J. Vahala, *Phys. Rev. Lett.* **94**, 223902 (2005); T.J. Kippenberg, H. Rokhsari, T. Carmon, A. Scherer, and K.J. Vahala, *Phys. Rev. Lett.* **95**, 033901 (2005).
- [3] J.D. Teufel, J.W. Harlow, C.A. Regal, and K.W. Lehnert, *Phys. Rev. Lett.* **101**, 197203 (2008).
- [4] S. Groblacher, J.B. Hertzberg, M.R. Vanner, G.D. Cole, S. Gigan, K.C. Schwab, and M. Aspelmeyer, *Nature Phys.* **5**, 485 (2009).
- [5] A. Schliesser, O. Arcizet, R. Riviere, G. Anetsberger, and T.J. Kippenberg, *Nature Phys.* **5**, 509 (2009).
- [6] Y.-S. Park and H. Wang, *Nature Phys.* **5**, 489 (2009).
- [7] M. Eichenfield, R. Camacho, J. Chan, K.J. Vahala, and O. Painter, *Nature (London)* **459**, 550 (2009).
- [8] W.H.P. Pernice, M. Li, and H.X. Tang, *Opt. Express* **17**, 12424 (2009).
- [9] F. Marquardt, J.P. Chen, A.A. Clerk, and S.M. Girvin, *Phys. Rev. Lett.* **99**, 093902 (2007).
- [10] I. Wilson-Rae, N. Nooshi, W. Zwerger, and T.J. Kippenberg, *Phys. Rev. Lett.* **99**, 093901 (2007).
- [11] M. Li, W.H.P. Pernice, and H.X. Tang, *Nat. Photon.* **3**, 464 (2009).
- [12] F. Elste, S.M. Girvin, and A.A. Clerk, *Phys. Rev. Lett.* **102**, 207209 (2009).
- [13] V. Giovannetti and D. Vitali, *Phys. Rev. A* **63**, 023812 (2001).
- [14] S. Fan, P.R. Villeneuve, J.D. Joannopoulos, and H.A. Haus, *Phys. Rev. Lett.* **80**, 960 (1998).
- [15] H.A. Haus, *Electromagnetic Noise and Quantum Optical Measurements*, Advanced Texts in Physics (Springer, Berlin, New York, 2000).
- [16] W.H.P. Pernice, M. Li, and H.X. Tang, *Opt. Express* **17**, 1806 (2009).
- [17] M.C. Cross, J.L. Rogers, R. Lifshitz, and A. Zumdick, *Phys. Rev. E* **73**, 036205 (2006).
- [18] G. Anetsberger, O. Arcizet, Q.P. Unterreithmeier, R. Riviere, A. Schliesser, E.M. Weig, J.P. Kotthaus, and T.J. Kippenberg, *Nature Phys.*, doi:10.1038/nphys1425 (2009).
- [19] M. Li, W.H.P. Pernice, C. Xiong, T. Baehr-Jones, M. Hochberg, and H.X. Tang, *Nature (London)* **456**, 480 (2008).
- [20] S. Groblacher, K. Hammerer, M.R. Vanner, and M. Aspelmeyer, *Nature (London)* **460**, 724 (2009).